ISSN 2959-6157

Research on Optimization Design of Electric Motor Based on Finite Element Calculation

Jianan You

Sichuan University,Chengdu,Sichuan Province,610000,China

Abstract:

With the widespread application of permanent magnet synchronous motors in the new energy vehicle market, the demand for verification and optimization of the design rationality of permanent magnet synchronous motors is gradually increasing. This article first establishes a three-phase four pole permanent magnet synchronous motor model based on the motor parameters provided by the motor manufacturer. Then, finite element simulation calculations are carried out on this model to solve the three-phase induced electromotive force, three-phase magnetic flux, cogging torque, iron core loss, and eddy current loss of the permanent magnet synchronous motor when it is unloaded. The rationality of the motor design is verified through the solution results. Finally, the average core loss of the permanent magnet synchronous motor is reduced by 3.6% through parameterized simulation, and its operating efficiency is improved. The optimization design is carried out on it.

Keywords: Permanent magnet synchronous motor; Parameterized simulation; Finite element calculation; optimal design

1 Introduction

New energy has the characteristics of lower carbon emissions, lower pollutant emissions, and more sustainable development, and is widely used in fields such as electric vehicles and new energy generation[1]. As the world's largest energy consumer and carbon emitter, vigorously developing new energy and related industries is an important way for China to achieve its goals of carbon peak and carbon neutrality. At the same time, electric motors play a crucial role in the development of new energy, especially in the application of new energy vehicles. Electric motors are the heart of new energy vehicles, responsible for driving the vehicle forward and being a key component of the vehicle's power output[2]. Therefore, improving motor efficiency and reducing losses are crucial for improving the power and economic performance of new energy vehicles. A large amount of research has been conducted by domestic and foreign scholars on the optimization of new energy vehicle motors. Reference [3] aims to reduce the manufacturing cost, cogging torque, no-load back electromotive force (THD), rated torque fluctuation, and electromagnetic vibration noise of permanent magnet synchronous motors. Reference [4] focuses on the optimization design of adding concave surfaces to the inner wall of the cooling water channel for permanent magnet synchronous motors. Through finite element method, the temperature situation of the motor under rated operating conditions is analyzed and compared before and after optimization, proving that the optimization improves the cooling effect of the motor. Reference [5] focuses on the built-in "V-type" rotor structure permanent magnet synchronous motor for vehicles. The presence of rotor auxiliary slots is selected as the optimization variable, and the stator iron loss is analyzed and optimized through finite element method combined with iron loss separation model. By designing the rotor auxiliary slots reasonably, the iron loss, harmonic content, and eddy current loss are reduced. Reference [6] redesigned the rotor structure of permanent magnet synchronous motors for A0 and A00 level electric vehicles, selecting the arrangement of permanent magnets and key rotor parameters as optimization variables. Through finite element analysis, torque ripple and cost were optimized, resulting in reduced torque ripple and improved torque cost-effectiveness. Reference [7] optimized the electromagnetic performance and temperature field of an oil cooled flat wire motor. Through two-dimensional and three-dimensional finite element models combined with fluid field simulation analysis, the segmented inclined pole and oil circuit structure of the rotor were selected as optimization variables to improve the heat dissipation efficiency of the motor, improve its electromagnetic performance, and reduce torque ripple and harmonic distortion rate. Refer-

ence [8] conducted sensitivity analysis on torque ripple of alternating pole permanent magnet motors, selecting pole arc coefficient and permanent magnet offset angle as optimization variables. Through finite element analysis combined with torque ripple theory, the performance of torque ripple was optimized to reduce torque ripple and electromagnetic vibration. Reference [9] focuses on the sensitivity analysis of rotor structural parameters for permanent magnet assisted synchronous reluctance motors used in electric vehicle drive. The number of magnetic barrier layers and permanent magnet content are selected as optimization variables, and the torque performance and weak magnetic speed regulation performance are optimized through finite element combined with analytical models, improving the electromagnetic performance and anti demagnetization ability of the motor. Reference [10] proposes a hybrid transposition flat wire winding structure for the flat wire winding of electric vehicle drive motors. By combining Leeds flat wire and solid flat wire, the AC loss is optimized, and the manufacturing of this winding is achieved through 3D printing technology. The results show that the motor losses are effectively reduced and the motor efficiency is improved in a wide frequency range. Reference [11] conducted a multi-objective sensitivity analysis on the structural size parameters of a doubly salient permanent magnet dual stator (DSPMDS) motor, selected key structural size parameters, and optimized the design using response surface methodology. Through finite element analysis and experimental verification, the optimized motor has achieved significant improvements in reducing torque fluctuations and iron core losses. Reference [12] proposes three optimization strategies for direct torque control of a four 2-phase 8/6-pole switched reluctance motor: subdivision of sectors, addition of magnetic flux state, and use of torque distribution function. Through finite element analysis combined with nonlinear dynamic model simulation verification, torque ripple is reduced and motor performance is improved. Reference [13] provides a third-order harmonic current flow circuit for three-phase permanent magnet synchronous motors, based on which optimization design is carried out. Through finite element model analysis and optimization, the performance of the motor drive system is improved, and the reliability and fault tolerance of the system are enhanced. Reference [14] optimized the design of an induction motor using the model reference adaptive method and alloy cross-section method, resulting in the optimal rotor flux level for machine operation. By reducing the indoor unit iron core loss, the efficiency of the drive system was improved. Reference [15] focuses on permanent magnet synchronous motors, selecting stator inner diameter, air gap length, armature calculation length, wire cross-sectional area, and pole arc coefficient as optimization variables. Through multi island genetic algorithm optimization design, energy consumption and power loss are reduced, and energy efficiency is improved. Reference [16] optimized the motor peak power and dynamic performance parameters of a dual motor power system based on the Simpson gear set. By minimizing the motor peak power to meet the dynamic performance requirements, and adopting a mode selection strategy to optimize energy efficiency, the energy efficiency of electric vehicles was improved. Reference [17] considers the overall driving cycle as a design optimization factor for permanent magnet motors used in electric vehicle applications, and optimizes their performance through an adaptive differential evolution algorithm combined with a two-dimensional finite element model. This improves the efficiency and torque quality of the motor, reduces power loss and torque ripple.

This article mainly conducts finite element analysis to verify the effectiveness of the design of a three-phase four pole permanent magnet synchronous motor, and optimizes its design through parametric simulation.

2 Simulation of Permanent Magnet Synchronous Motor Based on Finite Element Calculation

This section first focuses on the finite element modeling and mesh generation of three-phase quadrupole permanent magnet synchronous motor, and then verifies the three-phase induced electromotive force, magnetic flux, torque, iron core loss, and eddy current loss of three-phase quadrupole permanent magnet synchronous motor under no-load state through finite element solution.

2.1 Design parameters of permanent magnet synchronous motors

This section models three-phase quadrupole permanent magnet synchronous motors. Firstly, the rotor inner diameter, stator outer diameter, and other parameters of the motor are obtained from the motor manufacturer. Based on this model, finite element mesh generation is carried out to verify its basic parameters.

The stator of the established three-phase four pole permanent magnet synchronous motor is a double-layer full pitch winding, and its basic parameters are shown in Table 1:

Table 1 Basic parameters of three-phase four pole PMSM

Parameters	Sign	Value
Inner Diameter of Rotor(mm)		85
Outer Diameter of Stator(mm)		130
Core Length(mm)	L	145
Width of Air Gap(mm)	W	0.4
Number of Poles	p	4
Number of Stator Slots	Z	48
Polar Distance	τ	12
Pitch	y	10

In order to conduct finite element simulation on it, we counted the materials of its various components as shown in Table 2. The stator core and rotor core both used DW465_50 silicon steel plate model, while the stator conductor material was copper.

Table 2 Materials of Various Components of Three Phase Four Pole PMSM

Synchronous Motor Components	Material
Stator Core	DW465_50
Rotor Core	DW465_50
Stator Conductor	Copper
Permanent Magnet	P_mag
Stator Solving Region	Vacuum
Rotor Motion Area	Vacuum

Among them, the P_mag material is an improved permanent magnet material with a coercivity of -94700A/m and a residual magnetic induction strength of 1.25T. Based on the permanent magnet parameters provided by the manufacturer, the permanent magnet was manually modeled to complete the simulation.

The final established model diagram is shown in Figure 1:

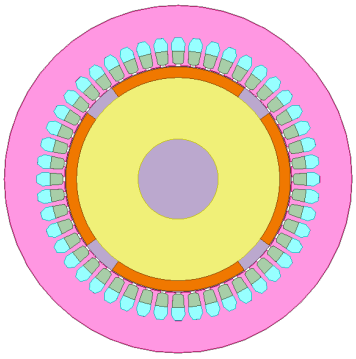

Figure 1 Model of three-phase four pole permanent magnet synchronous motor

2.2 Finite element simulation calculation of permanent magnet synchronous motor

In order to verify the rationality of such a motor design, this section conducts finite element analysis on it through Maxwell finite element solution system. In order to verify the parameters of the motor's current, torque, and other changes over time, and the three-dimensional model of the motor can be roughly regarded as the stretching of its two-dimensional model on the z-axis, we chose to analyze the type of two-dimensional transient field. As shown in Figure 2, this section first determines the basic parameters of the permanent magnet synchronous motor, and sets the length of the iron core according to the parameters. Then, the stator slot, stator iron core, stator winding, permanent magnet, rotor iron core, and motion boundary are gradually drawn (where the motion boundary includes the stator solution area and rotor motion area). Then, the materials of each component are set, and the relative coordinate system for the rotation of the four permanent magnets is set. Secondly, boundary conditions are set, and finally, the motion components are set with a corresponding speed of 1500r/min, completing the finite element modeling analysis of the permanent magnet synchronous motor.

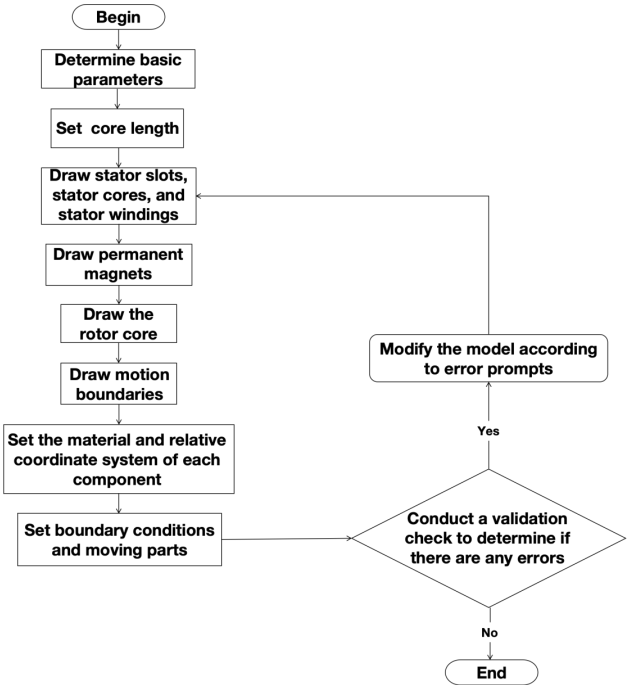

Figure 2 Finite Element Modeling Process Diagram

In order to balance the accuracy of the model and the computational power of the computer, the solution is set after self checking analysis, with a solution time of 0.2 seconds and a solution step of 0.001 seconds.

2.3 Analysis of simulation results

Based on the above solution settings, the finite element calculation solution results can be obtained.

The three-phase induced voltage obtained from the solution is shown in Figure 4. From the graph, it can be seen that the motor is three-phase symmetrical, and the three-phase induced voltage roughly follows a sinusoidal distribution. The maximum absolute value is about 244.29V, and the effective value is about 172.74V.

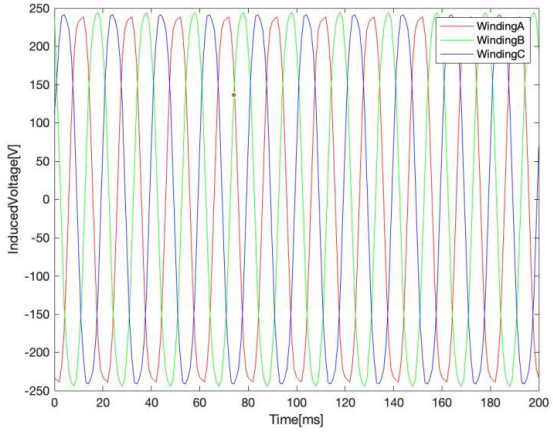

Figure 4 Three phase induced voltage curve

Due to the motor being in an unloaded state, its three-phase input current is zero.

The three-phase flux linkage obtained from the solution is shown in Figure 5. From the graph, it can be seen that the three-phase flux linkage also roughly follows a sinusoidal distribution, with a maximum absolute value of approximately 0.85Wb.

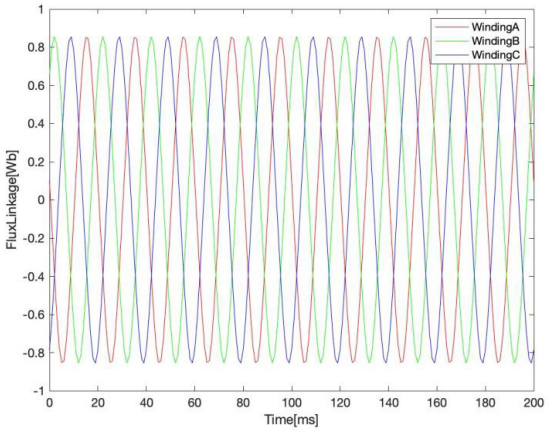

Figure 5 Three phase flux linkage curve diagram

The calculated cogging torque is shown in Figure 6. From the graph, it can be seen that it is a pointed wave with a maximum absolute value of approximately 4.34N·m, which overall meets our requirements for cogging torque.

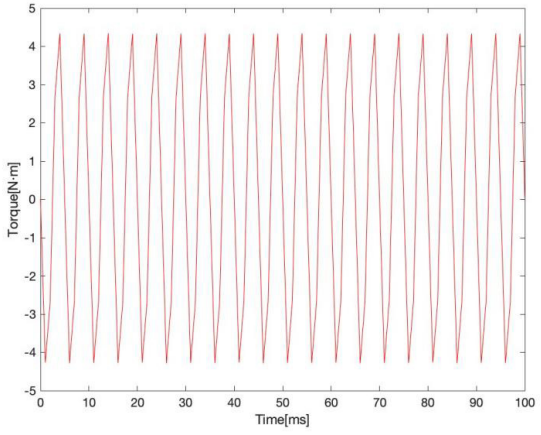

Figure 6 Cogging torque curve

The iron core loss and eddy current loss are shown in Figure 7. From the graph, it can be seen that the core loss gradually decreases after reaching its peak at the beginning, and the number and amplitude of curve fluctuations are greater than eddy current loss, with a maximum value of about 4.88mW and an average value of about 1.21mW; The waveform of eddy current loss is close to steady, with a maximum value of about 0.49mW and an average value of about 0.43mW.

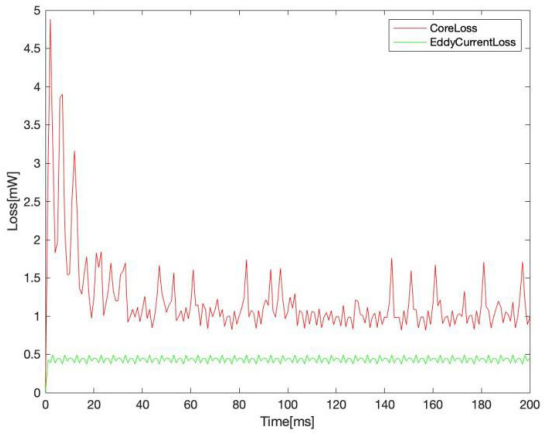

Figure 7 Core Loss and Eddy Current Loss Curve

The distribution map of magnetic field lines obtained by solving is shown in Figure 8, and the phenomenon of magnetic field line closure is good without magnetic leakage.

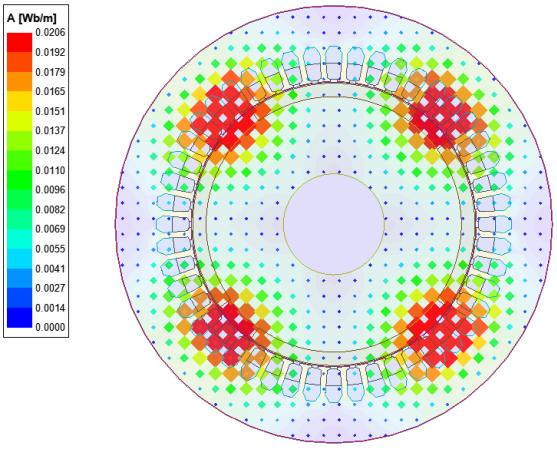

Figure 8 Distribution of magnetic field lines

The magnetic density distribution map is shown in Figure 9, with a maximum value of 3.056T and a minimum value of 0.2037T, which overall meets the motor design requirements.

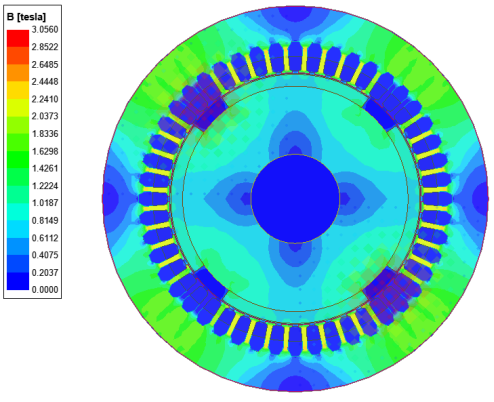

Figure 9 Magnetic density distribution map

From the above results, it can be concluded that the motor is three-phase symmetrical under no-load conditions, and its three-phase induced electromotive force, three-phase magnetic flux, torque, etc. meet our requirements.

3 Motor Optimization Design Based on Parameterized Simulation

This article conducts finite element modeling and mesh generation on a three-phase quadrupole permanent magnet synchronous motor, and verifies that its basic parameters meet the requirements. After that, parameterized simulation is carried out on the motor to optimize it and reduce motor losses. Due to the fact that motor losses vary with motor design parameters, and we have not obtained a specific relationship between motor losses and motor design parameters, in this section, we modified the stator outer diameter of the motor through finite element simulation experiments to complete parameterized simulation and verify its design requirements.

3.1 Parameterized simulation

For the parameterized simulation of three-phase quadrupole permanent magnet synchronous motor, the stator outer diameter of the motor model should be set as a variable to determine the range of stator outer diameter variation; Afterwards, the models with different stator outer diameters were analyzed, self checked, and solved. The solving time was still set to 0.2 seconds, and the solving step was still set to 0.001 seconds; Then, by solving, the corresponding iron core loss and eddy current loss for different stator outer diameters are obtained; Finally, by comparing the losses corresponding to different stator outer diameters, the influence of stator outer diameter size on motor losses is obtained. The flowchart is shown in Figure 10:

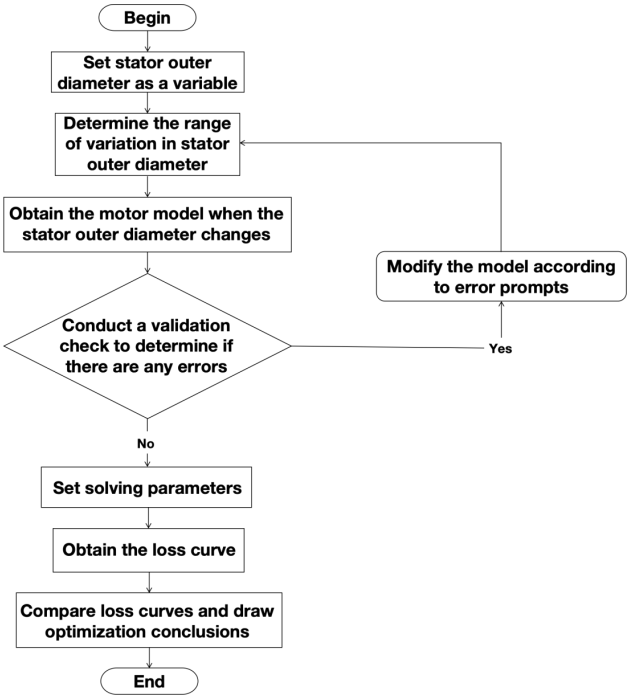

Figure 10 Parameterized simulation flowchart

3.2 Parameterized simulation results

The range of variation in stator outer diameter is 60-70mm, with a spacing of 2mm. After parameterized simulation, the results of core loss and eddy current loss are shown in Table 3:

Table 2 Parameterized simulation results

Stator Outer Diameter(R)	The maximum loss, average loss and minimum loss excluding origin	
R=60mm	Core Loss: maximum value is 4.4552mW minimum value is 0.7774mW average value is 1.1687mW	Eddy Current Loss: maximum value is 0.5091mW minimum value is 0.3461mW average value is 0.4288mW
R=62mm	Core Loss: maximum value is 4.4552mW minimum value is 0.7761mW average value is 1.1783mW	Eddy Current Loss: maximum value is 0.5091mW minimum value is 0.3461mW average value is 0.4288mW
R=64mm	Core Loss: maximum value is 4.4552mW minimum value is 0.7762mW average value is 1.1701mW	Eddy Current Loss: maximum value is 0.5091mW minimum value is 0.3461mW average value is 0.4288mW
R=66mm	Core Loss: maximum value is 4.4552mW minimum value is 0.7765mW average value is 1.1790mW	Eddy Current Loss: maximum value is 0.5091mW minimum value is 0.3461mW average value is 0.4288mW
R=68mm	Core Loss: maximum value is 4.4552mW minimum value is 0.7906mW average value is 1.1684mW	Eddy Current Loss: maximum value is 0.5091mW minimum value is 0.3461mW average value is 0.4288mW
R=70mm	Core Loss: maximum value is 4.4552mW minimum value is 0.7871mW average value is 1.1664mW	Eddy Current Loss: maximum value is 0.5091mW minimum value is 0.3461mW average value is 0.4288mW

The loss curves corresponding to stator outer diameters R of 60mm, 62mm, 64mm, 66mm, 68mm, and 70mm obtained from parameterized simulation are shown in Figures 11, 12, 13, 14, 15, and 16, respectively

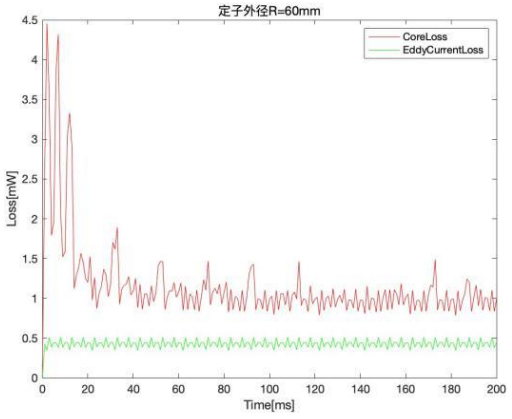

Figure 11 Loss Curve for R=60mm

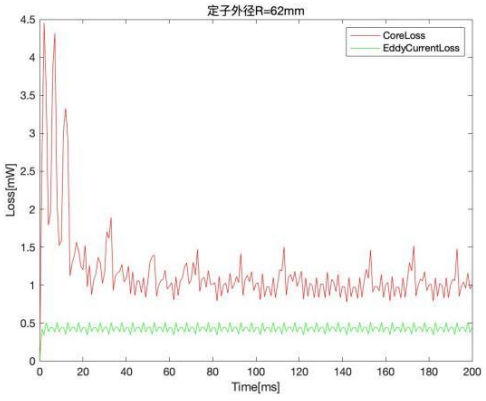

Figure 12 Loss Curve for R=62mm

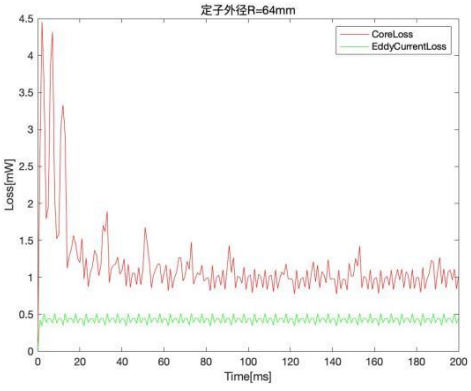

Figure 13 Loss Curve for R=64mm

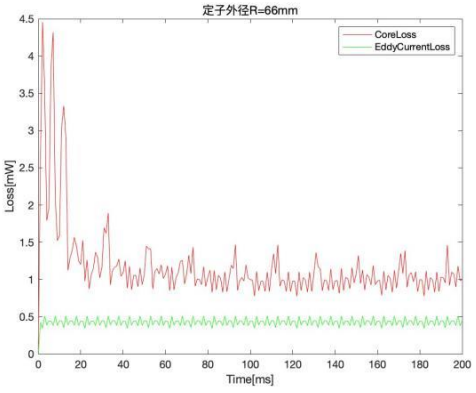

Figure 14 Loss Curve for R=66mm

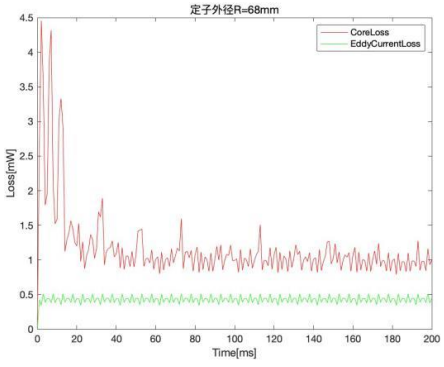

Figure 15 Loss Curve for R=68mm

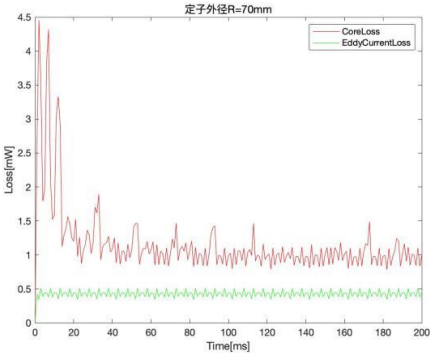

Figure 16 Loss Curve for R=70mm

From the above results, it can be seen that as a parameterized simulation with a stator outer diameter variation range of 60-70mm, the impact on eddy current loss is minimal, and the maximum, minimum, and average values are almost consistent, indicating that eddy current loss is less sensitive to the stator outer diameter; For the iron core loss, it has a significant impact compared to eddy current loss. Even though the maximum value is almost the same, the minimum and average values have changed. The results show that when the stator outer diameter is 70mm, the minimum and average values of the iron core loss are the highest, indicating that the fluctuation amplitude of the iron core loss is small and the overall loss is small. Compared with the average value of the iron core loss when the stator outer diameter is 65mm, the average value of the iron core loss decreases by 3.6%, and the

three-phase four pole permanent magnet synchronous motor is optimized.

4 Summary

This article focuses on a three-phase four pole permanent magnet synchronous motor. Firstly, the basic parameters such as stator outer diameter, rotor inner diameter, iron core length, and the materials of each component were determined, and finite element simulation was conducted to verify the effectiveness of its initial design. It was found that the effective value of the three-phase induced electromotive force was about 172.74V, the maximum value of the three-phase magnetic flux was about 0.85Wb, and the maximum absolute value of the cogging torque was about 4.34N·m. Furthermore, parameterized simulation was conducted on the three-phase four pole permanent magnet synchronous motor to optimize its design. It was found that when the outer diameter of the stator varied between 60mm and 70mm, and the outer diameter of the stator was 70mm, the corresponding iron core loss was relatively small. The average iron core loss was reduced by 3.6% compared to the outer diameter of the stator, which was 65mm.

References

[1]W. Yin, Development and Utilization of New Energy in Electric Power and Energy Conservation Measures under the Background of Sustainable Development Strategy, [J]. Automation Application, 2023, 64(S2):32-34.

[2]M. Lu, Y. Liu and B. Li, The Matching of E-motor Systems for NewEnergy Vehicles. [J].Automobile Applied Technology,2022,47(13):1-4.DOI:10.16638/j.cnki.1671-7988.2022.013.001.

[3]H. Huang, S. Hai, S. Wu, Optimization Design of Rotor Magnetic Steel Topology Structure of PMSM for New Energy Vehicle, [J]. Explosion-Proof Electric Machine, 2023,58(2):34-37.DOI:10.3969/J.ISSN.1008-7281.2023. 02.09.

[4]Z. Chen, X. Xiao, D. Hui, Heat dissipation analysis and heat dissipation structure optimization of permanent magnet synchronous motor for new energy vehicles[J]. Shanghai Auto, 2024(02): 3-8+21.

[5]H. Wang, Z. Jiang, P. Chao, ect, Analysis and Optimization of StatorIron Loss of Permanent Magnet Synchronous Motor for Vehicle, [J]. Electric Machines & Control Application,2021,48(9):96-102,109.DOI.10.12177/ emca.2021.073.

[6]X. Ju, F. Zhang, Y. Cheng, ect, Overview of Key Issues of Flat WireWinding of Traction Motor for Electric Vehicles, [J/OL].Proceedings ofthe CSEE:1-18[2024-03-10].http://kns.cnki.net/kcms/detail/11.2107.tm. 20230825.1219.007.html.

[7]Y. Fan, Calculation of Temperature Field and Optimization Design ofOil Circuit Structure of Motor With Hairpin Windings for New EnergyVehicles[D].Harbin University of Science and Technology, 2024.DOI:10.27063/d.cnki.ghlgu.2023.000702.

[8]G. Zhang, Design and Optimization of Low Torque Ripple Interior Consequent-pole Permanent Magnet Machine, [D]. Nanjing University of Aeronautics and Astronautics, 2023. DOI:10.27239/d.cnki.gnhhu.2021. 000492.

[9]L. Wu, Research of Rotor Structure of PMA-SynRM for Electric Vehicle Application, [D].Hubei University of Technology, 2020. DOI:10.27131/d. cnki.ghugc.2020.000362.

[10]Y. Chen, X. Zhu, L. Quan, ect, Parameter Sensitivity Optimization Design and Performance Analysis of Double-Salient Permanent-Magnet Double-Stator Machine, [J].Transactions of China Electrotechnical Society, 2017,32(08):160-168.DOI:10.19595/j.cnki.1000-6753.tces.2017. 08.019.

[11]D. Liu, A. Li, W. Liu, ect, Rotor optimization of permanent magnet-assisted synchronous reluctance motor for electric vehicles[J].Electric Machines and Control, 2022,26(09):119-129. DOI:10.15938/j.emc.2022.09.013.

[12]J. Bai, Research on Optimization of Direct Torque Control Strategy of Switched Reluctance Motor[D].Harbin Engineering University,2022. DOI: 10.27060/d.cnki.ghbcu.2021.000195.

[13]H. Liu, W. Fan, Q. Zuo and Y. Jiang, “Optimization design of three-phase permanent magnet synchronous motor drive system for electric vehicle,” 2021 IEEE Sustainable Power and Energy Conference (iSPEC), Nanjing, China, 2021, pp. 3417-3422, doi: 10.1109/iSPEC53008.2021.9735499.

[14]A. Pal and S. Das, “A new sensorless speed estimation strategy for induction motor driven electric vehicle with energy optimization scheme,” 2016 IEEE 1st International Conference on Power Electronics, Intelligent Control and Energy Systems (ICPEICES), Delhi, India, 2016, pp. 1-6, doi: 10.1109/ICPEICES.2016.7853077.

[15]D. Wei, H. He and J. Li, “A Computationally Efficiency Optimal Design for a Permanent Magnet Synchronous Motor in Hybrid Electric Vehicles,” 2020 IEEE 9th International Power Electronics and Motion Control Conference (IPEMC2020-ECCE Asia), Nanjing, China, 2020, pp. 43-47, doi: 10.1109/IPEMC-ECCEAsia48364.2020.9367752.

[16]X. Hong, J. Wu and N. Zhang, “Parameters Design and Energy Efficiency Optimization of a New Simpson Gearset based Dual Motor Powertrain for Electric Vehicles,” 2021 60th Annual Conference of the Society of Instrument and Control Engineers of Japan (SICE), Tokyo, Japan, 2021, pp. 685-690.

[17]A. G. Sarigiannidis, M. E. Beniakar and A. G. Kladas, “Fast Adaptive Evolutionary PM Traction Motor Optimization Based on Electric Vehicle Drive Cycle,” in IEEE Transactions on Vehicular Technology, vol. 66, no. 7, pp. 5762-5774, July 2017, doi: 10.1109 /TVT. 2016.2631161.